CRYSTAL GROWTH & DESIGN

pubs.acs.org/crystal

Article

On the Role of Dioxane in the Synthesis of In-Derived MOFs

Caleb J. Tatebe, Saidah Yusuf, Michael K. Bellas, Matthias Zeller, Christopher Arntsen, and Douglas T. Genna*

Cite This: *Cryst. Growth Des.* 2021, 21, 6840−6846

Read Online

ACCESS | Metrics & More | Article Recommendations | Supporting Information

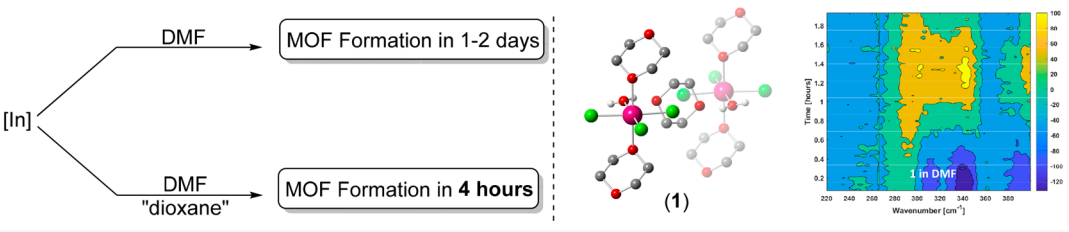

ABSTRACT: The role of the solvent in the synthesis of metal−organic frameworks (MOFs) is often as complex as the MOF itself. In MOF syntheses, solvents, typically polar formamides, can act as solubilizing agents, ligands for the metal centers, and chemical reagents. Further compounding this complexity, MOFs are often synthesized in solvent mixtures. Several In-derived MOFs have been synthesized using a DMF/dioxane solvent mixture. A combination of synthetic, spectroscopic, and computational methods was used to understand the synergy between DMF and dioxane in the synthesis of In-derived MOFs MIL-68, QMOF-2, ATF-1, and ZJU-28. These studies revealed the following. (1) Dioxane plays a critical role in the bulk solvent (lowering the dielectric constant) and as a ligand directly coordinating to In. (2) While $InCl_3$ can spontaneously form $[InCl_4]^-$ and $[InCl_2(solv)_4]^+$ in many polar solvents, Raman spectroscopy revealed that this transformation does not occur in DMF. (3) A new indium solvato polymer, $InCl_3(dioxane)_2(H_2O)$ (**1**), was isolated and demonstrated to be an effective In source, yielding MIL-68 in 5 h at 120 °C.

INTRODUCTION

Metal−organic frameworks (MOFs) are materials made up of inorganic and organic building units that self-assemble, forming porous two- or three-dimensional crystalline arrays.[1] Permanent porosity and tunable functionality have led to MOFs being implemented in applications such as gas storage, catalysis, drug delivery, and toxicant removal, among others.[2−7] Despite the success of MOFs in these varied applications, MOF formation is not a fully understood process. In solution not only do the inorganic and organic components have to self-assemble to a critical mass capable of nucleation but often also the inorganic molecular building unit (MBU) itself must form from simple inorganic starting materials. To further complicate matters, many metals can yield multiple molecular/secondary building units (SBUs). For example, indium along with the other group 13 metals (Al, Ga) can access at least three different MBU/SBU combinations: anionic $[In(O_2CR)_4]^-$, a neutral $[In(\mu\text{-}O_2CR)_2(\mu\text{−}OH)]_\infty$ infinite chain, and cationic $[In_3O(O_2CR)_6(H_2O)_3]^+$. Often the control of these synthetic outcomes is restricted to the careful control of the mole fraction of the inorganic and organic components.[8] Other routes involve presynthesizing the MBU[9] or developing the perfect cocktail of reagents, solvents, and temperatures; often by Edisonian experimentation.[10−13]

Due to the complexity of MOF synthesis, a multifaceted and nuanced approach is necessary to fully understand the formation of MOFs during both pre- and postnucleation. Many studies have focused on using X-ray crystallography and microscopy techniques to understand nucleation and growth proceses.[14−16] Solution-phase studies date back to Ferey's seminal work using ^{27}Al NMR, which established that the Al SBU is present in solution during the self-assembly of MIL-96 and MIL-110, respectively.[17] However, due to the high nuclear spin state (and often quadrupolar nature) of most inorganic nuclei found in MOFs, NMR has not been proven to be a universal technique for solution-phase MOF studies. Recently, vibrational spectroscopy has been established as a general technique to interrogate the formation of Al-derived infinite chains[18−20] and defective Zr_6 clusters,[21,22] respectively.

The solvent is the most commonly varied component during the Edisonian exploration of MOF synthesis. To the outside observer and the practitioner alike, the choice of solvent in the synthesis of MOFs appears to be a choice between dimethylformamide (DMF) or some arbitrary multicomponent DMF-containing mixture. What is the role of the solvent in the synthesis of MOFs? Is it simply to solubilize the components

Received: July 2, 2021
Revised: October 27, 2021
Published: November 11, 2021

https://doi.org/10.1021/acs.cgd.1c00766
Cryst. Growth Des. 2021, 21, 6840−6846

allowing for chemical transformations to take place? Yet solvent-free mechanochemical synthesis has taught us that a solvent is not always necessary for MOF synthesis.[23−26] Could the solvent be serving as a ligand place holder for the polymerizing organic strut component, a concept previously reserved[27] only for carboxylic acid modulators? Coordination and organometallic chemistry have taught us the importance of reversible binding of solvato ligands in inorganic transformations as well as in transition-metal catalysis mechanisms.[28,29] Could the solvent be playing multiple roles in MOF synthesis? Putatively, DMF has multiple functions in a MOF synthesis. Not only does DMF solubilize the reaction components but it also acts as a chemical reagent with its decomposition into Me_2NH and CO (or formic acid/formate)[30,31] being critical to the formation of anionic MOFs that require a charge-balancing $[Me_2NH_2]^+$ counterion. Formate, itself, often acts as an *in situ* modulator in the synthesis of Zn- and Zr-derived MOFs.[32] Additionally, DMF is a known ligand for many metals used in MOF synthesis.[27,33,34] If a single component solvent system such as DMF can have such a potentially sophisticated role in MOF synthesis, then what about systems with multiple solvents? Studies regarding the effects of solvent-level quantities of additives in UiO-66 synthesis reveal that acidic additives have drastic effects on the initial formation of the Zr_6 cluster as well as on the ligand exchange chemistry necessary for self-assembly.[14,35,36]

Our laboratory has used a 3/2 (v/v) DMF/dioxane solvent mixture for the synthesis of In-derived MOFs extensively due to high yields and the formation of higher quality crystalline materials compared to DMF-only systems.[37−39] To our knowledge the first reported use of dioxane as a cosolvent in the synthesis of In-derived MOFs was by Chen and Qian for the synthesis of ZJU-28.[40] While the use of dioxane in our hands routinely yielded materials with higher crystallinity, the origin of this effect was unknown and warranted further investigation. To study this multisolvent system, we targeted MOFs that were robust enough to allow for synthesis in both single and multicomponent solvent systems. Herein we report a systematic study on the effect of dioxane as a cosolvent with DMF in the synthesis of select In-derived MOFs from $InCl_3(H_2O)$.

RESULTS AND DISCUSSION

It is widely accepted that when $InCl_3$ is dissolved in polar solvents it converts into anionic $[InCl_4]^-$ and a cationic In species, the structure of which is the subject of debate but is most likely $[InCl_2(solv)_4]^+$ (eq 2).[33,41−43] We initially

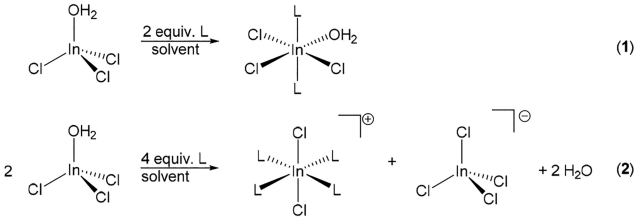

hypothesized that dioxane could be affecting the formation of $[InCl_4]^-$ and $[InCl_2(solv)_4]^+$ upon the dissolution of $InCl_3(OH_2)$ and thus have a downstream effect on self-assembly. To this end we studied the solution-phase behavior of $InCl_3(OH_2)$ in DMF, dioxane, DMF/dioxane, tetrahydrofuran (THF), and acetone *in situ* using Raman spectroscopy and *in silico* using density functional theory (DFT) with implicit solvent models.

All solution-phase DFT calculations were conducted using the ωB97X-D[44,45] functional and 6-316G* basis set for all non-In atoms, while the LANL2DZ-SV basis set was used for In[46] using the Spartan 18 program with implicit solvent models at 298.15 K. To this end we studied the behavior of $InCl_3(H_2O)$ in the presence of coordinating solvent ligands in implicit solvent *in silico*. We used $InCl_3(H_2O)$ and not $InCl_3$ because thermogravimetric analysis reveals that there is one water molecule per In atom in our $InCl_3$ (Figure S1). The formation of *mer*-$InCl_3$(*trans*-solv)$_2(H_2O)$ from $InCl_3(H_2O)$ was examined (eq 1; the results are summarized in Table 1) and in all

Table 1. Summary of Computational Data for $InCl_3(OH_2)$ Solvation (Eq 1) vs Formation of $[InCl_4]^-$ and $[InCl_2(solv)_4]^+$ (Eq 2)

ligand	solvent	ΔH (eq 1) (kcal/mol)	ΔH (eq 2) (kcal/mol)
DMF	DMF	−45.9	−62.6
dioxane	dioxane	−40.1	−10.3
dioxane	DMF	−37.5	−1.9
THF	THF	−41.7	−50.3
acetone	acetone	−35.0	−39.3

cases the formation of the octahedral solvate was enthalpically favored. Second, we studied the formation of $[InCl_4]^-$ and $[InCl_2(solv)_4]^+$ from the solvated octahedral complex itself (Table S2). Note that the optimal structure of $[InCl_2]^+$ was found to be [*trans*-$InCl_2(solv)_4]^+$ with all solvents studied. In all cases the formation of $[InCl_4]^-$ and $[InCl_2(solv)_4]^+$ was enthalpically disfavored from the octahedral solvate. Finally, we studied the formation of $[InCl_4]^-$ and $[InCl_2(solv)_4]^+$ directly from $InCl_3(H_2O)$ in the presence of implicit solvent (eq 2; the results ae summarized in Table 1). In these cases, the transformation was enthalpically downhill. A comparison of these pathways indicates that, starting from $InCl_3(H_2O)$ in DMF, THF, and acetone, the formation of $[InCl_4]^-$ and $[InCl_2(solv)_4]^+$ is the enthalpically favored pathway; however, when dioxane is present, either by itself or as a solution in DMF, the formation of the octahedral solvate is enthalpically favored over the formation of $[InCl_4]^-$ and $[InCl_2(solv)_4]^+$ *in silico*.

To further interrogate the behavior of $InCl_3(H_2O)$ in solution, *in situ* Raman data of $InCl_3(H_2O)$ dissolved in DMF, dioxane, DMF/dioxane (3/2 v/v), THF, and acetone, respectively, at 65 °C were collected (Figure 1) and compared with the *in silico* studies. In THF and acetone at 65 °C, $[InCl_4]^-$ formed immediately (determined by observation of a peak at 317 cm^{-1})[43,47] and no solvated form of $InCl_3$ (peaks range from 282 to 290 cm^{-1})[48] could be observed, consistent with our calculations. However, in DMF and DMF/dioxane (3/2 v/v) at 65 °C only minor amounts of $[InCl_4]^-$ are present. Surprisingly, in dioxane at 65 °C, peaks corresponding to solvated $InCl_3(OH_2)$ emerge at 40 min but rapidly disappear with the concomitant formation of $[InCl_4]^-$. The formation of $[InCl_4]^-$ in dioxane is reversible, as can be seen in the Raman spectra upon cooling (Figure S23). A new $InCl_3$-derived compound also precipitated, which a single-crystal X-ray diffraction analysis revealed to be $InCl_3(dioxane)_2(H_2O)$ (**1**) (Figure 2). The structure of **1** is a one-dimensional solvato coordination polymer in which the three Cl ligands adopt a meridional geometry and the dioxane ligands are *trans* to each

https://doi.org/10.1021/acs.cgd.1c00766
Cryst. Growth Des. 2021, 21, 6840−6846

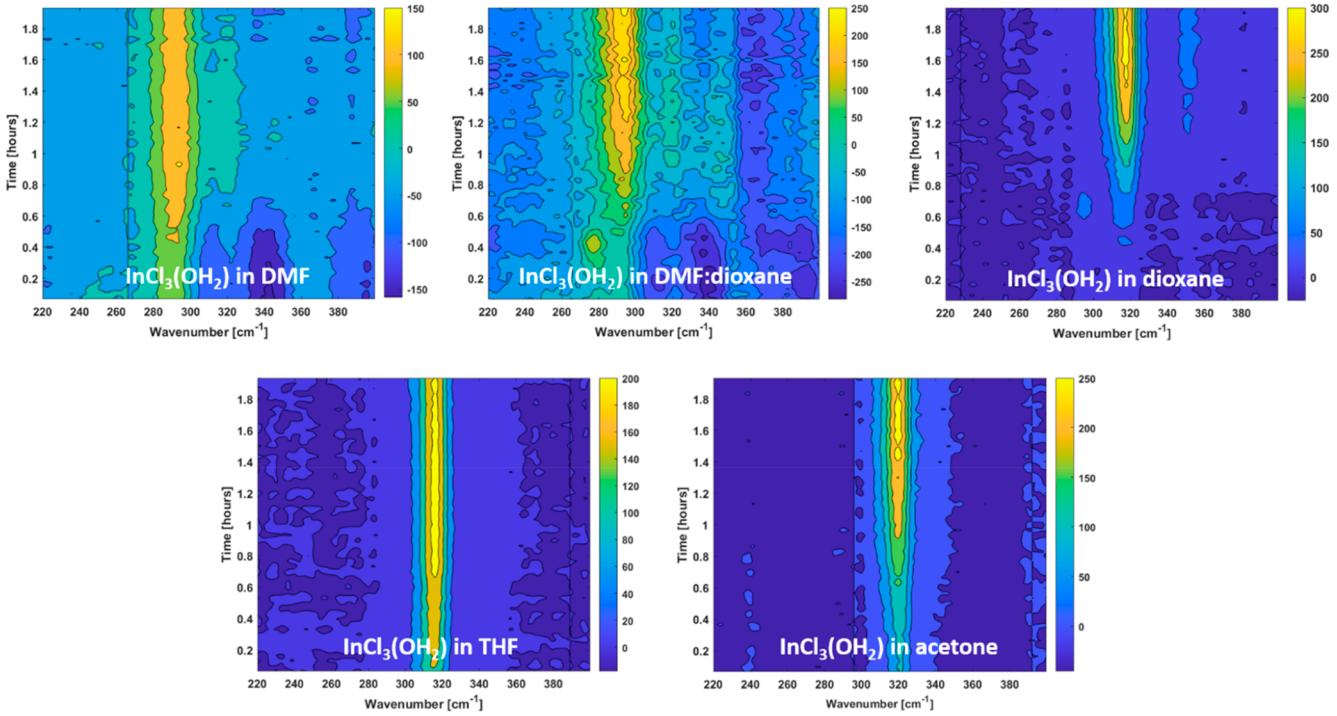

Figure 1. Two-dimensional contour plots of Raman data of $InCl_3(OH_2)$ in DMF, DMF/dioxane (3/2 v/v), dioxane, THF, and acetone incubated at 65 °C for 2 h.

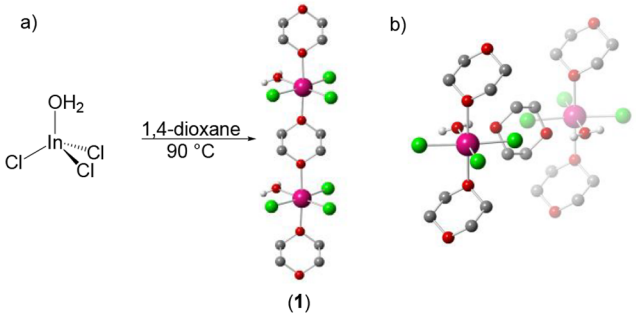

Figure 2. (a) Synthesis of 1-D solvato polymer **1**. (b) Cross-linking of 1-D chains with dioxane.

other, allowing for one-dimensional polymerization. Each 1-D chain is cross-linked through hydrogen bonding of the aqua ligand with an interstitial dioxane molecule. Additionally, **1** can be routinely synthesized by simple recrystallization of $InCl_3(H_2O)$ in dioxane at 90 °C.

While the solvation of $InCl_3(H_2O)$ was studied extensively, the solvation of the carboxylate was also investigated *in silico* using classical molecular dynamics. In these studies the solvation of formate, a computationally affordable substitute for terephthalate, in DMF, dioxane, and 1/1 DMF/dixoane was examined. These molecular dynamics simulations revealed that (1) the first solvation shell (at 3.5 Å) around formate in the DMF/dioxane mixture is predominantly DMF (1.8/1) and (2) at close contact (<2.5 Å) DMF is 3 times more likely to coordinate to the formate oxygen atoms. When they are taken in totality, these simulations indicate that the solvation of formate and thus its ability to interact with indium are not affected by the changes in DMF/dioxane mole fraction examined in this work.

The evidence of reversible formation of $[InCl_4]^-$ and $[InCl_2(solv)_4]^+$ (eq 2) in dioxane, when it is contrasted with

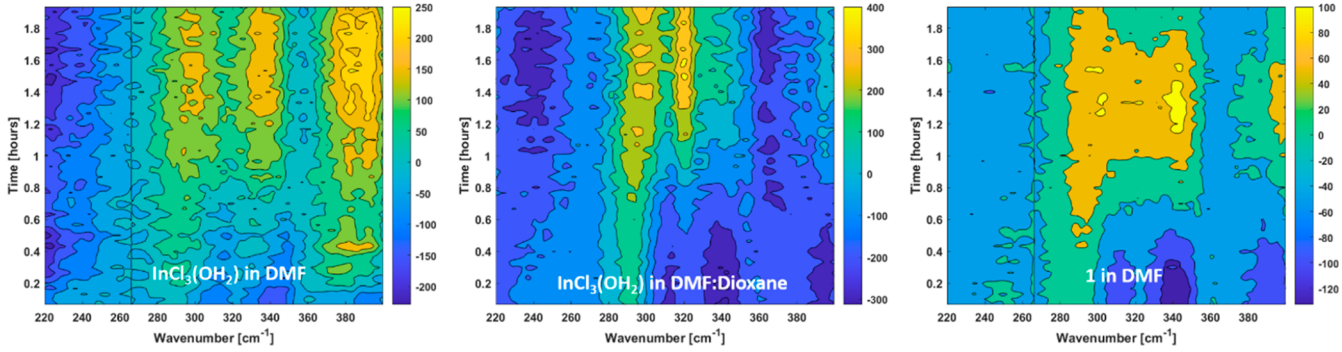

Figure 3. Two-dimensional contour plots of Raman data of $InCl_3(OH_2)$ in DMF and DMF/dioxane (3/2 v/v) and compound **1** in DMF at 120 °C for 2 h.

https://doi.org/10.1021/acs.cgd.1c00766
Cryst. Growth Des. 2021, 21, 6840−6846

our *in silico* studies, implies that, although the process may be enthalpically less favorable than solvation (eq 1), it has a lower kinetic barrier and this is observable *in situ*. While these findings are significant since they demonstrate that $[InCl_4]^-$ does not form at 65 °C in DMF, most In-derived MOFs are formed at temperatures above 100 °C and the behavior of $InCl_3(H_2O)$ in DMF may be different at elevated temperatures. To this end the formation of $[InCl_4]^-$ and $[InCl_2(solv)_4]^+$ in DMF and DMF/dioxane (3/2 v/v) was studied via *in situ* Raman spectroscopy at 120 °C (Figure 3). In DMF, a set of two vibrations at 337 and 385 cm^{-1}, which we tentatively attribute to In-coordinated DMF ligands, red-shifted with respect to free DMF vibrations at 353 and 404 cm^{-1}. In 3/2 DMF/dioxane a clear vibration at 320 cm^{-1} forms after 1 h, corresponding to $[InCl_4]^-$ formation. There are still significant vibrations for solvated $InCl_3$ at 297 cm^{-1} and the emergence of some less intense vibrations at 338 and 396 cm^{-1}, respectively. The Raman data collected with **1** dissolved in DMF at 120 °C are a hybrid of the individual $InCl_3(OH_2)$ in DMF and DMF/dioxane experiments. There are vibrations at 302, 320, 343, and 395 cm^{-1}. Vibrations at 343 and 395 cm^{-1} are still attributed to DMF coordinated to In; however, the presence of dioxane bound to In either directly or in solution is causing a smaller red shift of the vibrations relative to free DMF in solution. These data imply that, in DMF, the formation of $[InCl_4]^-$ can only occur in detectable amounts when dioxane is present. Since In-derived MOFs can form in DMF at 120 °C, the formation of $[InCl_4]^-$ and $[InCl_2(solv)_4]^+$ of $InCl_3$ does not appear to be necessary for In-derived MOF formation.

The serendipitous discovery of compound **1** led us to investigate whether it is present during the synthesis of In-MOFs with dioxane as a cosolvent. However, distinguishing between $InCl_3(H_2O)$ solvated with either DMF or dioxane by Raman spectroscopy is difficult due to the overlap of the In−Cl vibrations in the solvated $InCl_3(H_2O)$ region (290−295 cm^{-1}). Further complicating the interpretation of this region, the solvated structure of $InCl_3(H_2O)$ is most likely a dynamic mixture of solvato complexes. To complement the above Raman studies, the synthesis of In-derived MOFs using compound **1** and $InCl_3(H_2O)$ was examined, focusing on defining the induction period necessary to achieve a crystalline material and the crystallinity of the formed MOFs.

The induction periods were determined for the synthesis of anionic MOFs ATF-1, ZJU-28, and QMOF-2, which contain the $[In(CO_2R)_4]$ SBU, as well as MIL-68 containing the neutral $In(\mu\text{-}O_2CR)_2(\mu\text{-}OH)$ SBU at 100 and 120 °C using $InCl_3(H_2O)$ in DMF, $InCl_3(H_2O)$ in DMF/dioxane (3/2 v/v), and compound **1** in DMF along with the appropriate organic linker. The results of these studies are summarized in Table 2. Note that the induction period here is defined as the time in which enough MOF (a few milligrams) has precipitated for a powder X-ray diffraction (PXRD) analysis. These times were determined as an average of at least three trials performed by two separate individuals, who did not have knowledge of one another's time points. At 120 °C the addition of dioxane as a cosolvent did not lead to quicker induction times but did yield higher-quality crystalline material as determined by PXRD analysis (Figures S4, S6, S8, and S10). In this context, quality of crystalline material is defined as being phase pure and having narrow reflections in the powder X-ray diffractogram. When compound **1** was used, quicker induction times were observed for all MOFs tested and in some cases were 4−5 times earlier

Table 2. Induction Periods in Hours as a Function of Solvent and Indium Source[a]

	induction periods to achieve crystalline material (h)		
MOF	$InCl_3(H_2O)$ in DMF	$InCl_3(H_2O)$ in DMF/diox	**1** in DMF
ZJU-28	17(1)	22(5)	5.0(0.2)
ATF-1	17(2)	19(3)	13(4)
QMOF-2	18(2)	16(4)	12(2)
MIL-68	17(1)	18(1)	4.0(0.5)

[a]Note that all values are an average of at least three runs. Standard errors are given in parentheses.

without sacrificing crystal quality (Figures S4, S6, S8, and S10). At 100 °C, while some induction enhancements were observed with dioxane as a cosolvent or ligand (**1**), the results, regardless of the presence or absence of dioxane, were both highly variable and irreproducible, while the isolated MOFs were of generally poor crystal quality (Table S1 and Figures S5, S7, S9, and S11). This level of irreproducibility is attributed to the number of competing pathways that are possible at 100 °C, which is most notable when the syntheses of MIL-68 and QMOF-2 are compared. Both MOFs are derived from terephthalic acid and In but contain different inorganic nodes, an In-infinite chain (MIL-68) and $[In(CO_2R)_4]^-$ (QMOF-2). At 100 °C mixtures of the two materials are obtained regardless of the presence or absence of dioxane, implying that these two chemically different inorganic building units are present in solution and compete for resources. However, at 120 °C, the outcome is controlled more readily by stoichiometry, and the stoichiometrically disfavored species does not reach the critical concentration necessary for MOF formation. For example, the infinite-chain-derived MIL-68 can be isolated in 4 h using **1**, while it takes 12 h for QMOF-2 to form when compound **1** is used as the In source. This implies that the preformed dioxane solvate has a greater influence over the formation of the infinite chain in comparison to the formation of $[In(CO_2R)_4]^-$.

While empirically it is clear that dioxane influences the induction period necessary for crystalline MOF formation and the quality of the crystals formed, the cause is unclear. Dioxane has the potential to modify MOF formation in a number of ways. Each different way could enhance or detract from MOF formation by working either in consort or independently. We propose the following hypotheses for the observed dioxane-induced enhancement and report our attempts to support and/or disprove their existence and effect on MOF formation.

(1) Assuming that an $InCl_3(H_2O)(solv)_2$ complex forms upon dissolution (e.g., **1**), dioxane ligands in $InCl_3(H_2O)(diox)_2$ are more prone to being displaced by linkers in comparison to the DMF ligands in $InCl_3(H_2O)(dmf)_2$.
(2) Dioxane added to DMF lowers the dielectric constant, decreasing the solubility of the self-assembled products, leading to shorter induction periods necessary for MOF formation.
(3) Since self-assembly requires the ability to repair mistakes, dioxane could assist in the repair mechanism by facilitating Cl^-/carboxylate ligand exchange.
(4) Consistent with the one-dimensional polymer solid-state structure of compound **1**, dioxane could preorder the In centers, allowing for more rapid self-assembly.

https://doi.org/10.1021/acs.cgd.1c00766
Cryst. Growth Des. 2021, 21, 6840−6846

Hypothesis 1. We have calculated that the most likely "first intermediate" of $[In(CO_2R)_4]^-$ formation is the anionic species $[InCl_3(CO_2R)_4]^-$ (**I**).[49] Since **I** is an early-stage intermediate, its formation could be dependent on the initial solvent environment at In, meaning that it could be more favorable for the linker to displace dioxane versus DMF. This particular linker displacement was studied *in silico* (Figure 4),

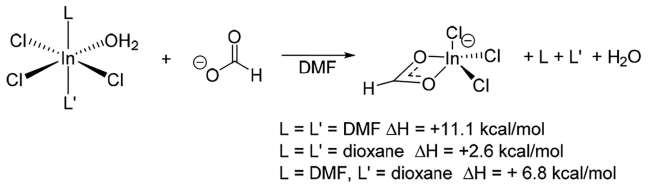

Figure 4. Summary of computational analysis on the formation of $[In(CO_2H)Cl_3]^-$.

again using formate as a computationally affordable substitute for terephthalate, and it was found that when L = L′ = DMF it is 11.1 kcal/mol enthalpically uphill, while when L = L′= dioxane it is 2.6 kcal/mol uphill. Additionally, when there is one dioxane and one DMF ligand, it is 6.8 kcal/mol uphill. These results imply that it is more enthalpically favorable to displace dioxane from In in comparison to DMF. The favorability of dioxane displacement can be attributed to the fact that DMF is a stronger Lewis base than dioxane[50] and thus it binds more tightly to In. Additionally, the cone angles for the In-dioxane and In-DMF ligands are 82 and 50° respectively, suggesting that dioxane has increased ligand lability, in comparison to DMF, for both electronic and steric reasons. By preforming the more labile In−dioxane bonds with compound **1**, MOF-node formation could be expedited relative to that when the synthesis is performed using pure DMF conditions.

Hypothesis 2. In order to study the effect of dielectric constant on the induction period, we targeted toluene as an appropriate cosolvent to replace dioxane. First, toluene has a dielectric constant of 2.4, while 1,4-dioxane has a dielectric constant of 2.2.[51] Second, toluene has a boiling point similar to that of dioxane (110 °C vs 101 °C) and lacks the ability to coordinate directly to the metal. Finally, the use of toluene does not affect the homogeneity of the start of the reaction. Any perturbation of the reaction in comparison to DMF should be attributable to changes in dielectric constant. To this end, when QMOF-2 was synthesized in DMF/toluene (3/2 v/v), MOF formation had an average induction period of 19(±2) h (compared to 16(±4) h in DMF/dioxane), while the high quality of crystallinity was retained as seen in DMF/dioxane (Figure S12). However, attempts to synthesize MIL-68 in DMF/toluene solvent yielded product mixtures that were mostly QMOF-2 (Figure S13). From these results it can be inferred that the change in dielectric constant is not the sole cause of dioxane's effects on the synthesis of In-derived MOFs and that dioxane is most likely coordinating directly to the In center.

Hypothesis 3. The ability of DMF or dioxane to facilitate self-assembly repair mechanisms was studied *in silico* by calculating the energy of solvent/carboxylate ligand exchange in DMF using the reaction in Figure 5. These studies revealed that when the solvato ligand is dioxane $\Delta H = -0.2$ kcal/mol and when the solvato ligand is DMF $\Delta H = 7.1$ kcal/mol. These data imply that, unlike DMF, dioxane, as indicated by the near-

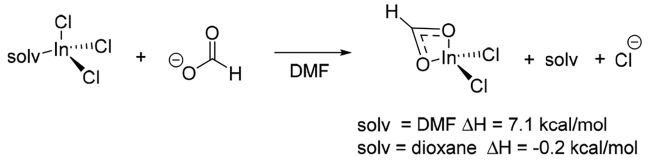

Figure 5. Summary of the computational analysis of solvent-assisted formate−chloride ligand exchange.

zero enthalpic barrier, can effectively assist chloride in carboxylate displacement repair steps of In-derived MOF formation. This would explain the qualitative increase in MOF crystallinity when dioxane is used as a cosolvent. Additionally, when compound **1** is used to synthesize MIL-68, QMOF-2, or ZJU-28 in the presence of DMF/dioxane (3/2 v/v) solvent, longer induction periods were observed and the crystal quality was poor to amorphous (Figures S16−S19). This is consistent with the low enthalpic barrier to dioxane/carboxylate ligand exchange. The presence of excess dioxane, once dioxane is bound to indium, prohibits carboxylate binding and drives the equilibrium to favor the In−dioxane and In−Cl bonds. To further support this, compound **1** was used in the synthesis of QMOF-2 and MIL-68 in a DMF/toluene solvent mixture. The MOFs were synthesized with average induction times of 20(±4) and 15(±1) h, respectively (Table S1), and retained a high quality of crystallinity.

Hypothesis 4. Due to the polymeric nature of the solid-state structure of **1**, we hypothesized that dioxane could be self-assembling/preordering In subunits prior to organic ligand exchange. To test this hypothesis, dioxane was replaced with tetrahydropyran (THP) in the synthesis of MIL-68 and QMOF-2, respectively. THP should coordinate to $InCl_3(H_2O)$ similarly to dioxane but would be unable to form the extended solvato coordination polymer due to its single oxygen atom. Syntheses of QMOF-2 using DMF/THP (3/2 v/v) as the solvent at 120 °C yielded an MOF with high crystal quality with an average induction period of 36 h. However, attempts to synthesize MIL-68 in DMF/THP solvent largely led to product mixtures of QMOF-2 and MIL-68 (Figures S14 and S15). Why the synthesis of MIL-68 is sensitive to solvent changes (e.g., DMF/toluene and DMF/THP) is unclear but could be related to the fate of the aqua ligand, which is necessary for the formation of the infinite chain.

CONCLUSIONS

The role of solvents in any given MOF synthesis is a balance between providing proper solvation of the reagents and intermediates formed during self-assembly and allowing the polymeric material to nucleate and grow. Polar solvents can serve as displaceable ligands for the metal center, providing a scaffold for at-metal repair mechanisms to assist in the self-assembly process. When they are taken in totality, the data present the complex role of dioxane as an additive in the synthesis of In-derived MOFs. In this study, and specifically for MOFs synthesized from $InCl_3$, 1,4-dioxane complements the traditional DMF solvent in several ways. Since 1,4-dioxane contains two metal-coordinating sites, it allows for a level of preassembly or self-assembly assistance for the indium building units. However, this preassembly is only afforded to compound **1**. When $InCl_3(H_2O)$ is in DMF/dioxane solvent, DMF is the enthalpically preferred solvato ligand, meaning that only small quantities of dioxane are bound to indium at any point of the

https://doi.org/10.1021/acs.cgd.1c00766
Cryst. Growth Des. 2021, 21, 6840−6846

reaction coordinate. While this allows for dioxane to act as an effective self-assembly repair agent (perhaps even after the first carboxylate binding event), it does not allow for preordering in solution. This proposed repair mechanism leads to increases in crystal quality. Shorter induction periods can be attributed to preordering in solution of the In centers as evidenced by the onset acceleration when compound **1** is used and are not due to changes in the dielectric constant of the solvent mixture. Thus, it should not be lost that the solvato polymer **1** is a new starting material that leads to rapid, highly crystalline In-derived MOFs.

■ ASSOCIATED CONTENT

Supporting Information

The Supporting Information is available free of charge at https://pubs.acs.org/doi/10.1021/acs.cgd.1c00766.

Synthetic and spectroscopic experimental details and single crystal X-ray, PXRD, TGA, and Raman data (PDF)

Accession Codes

CCDC 2091372 contains the supplementary crystallographic data for this paper. These data can be obtained free of charge via www.ccdc.cam.ac.uk/data_request/cif, or by emailing data_request@ccdc.cam.ac.uk, or by contacting The Cambridge Crystallographic Data Centre, 12 Union Road, Cambridge CB2 1EZ, UK; fax: +44 1223 336033.

■ AUTHOR INFORMATION

Corresponding Author

Douglas T. Genna − *Department of Chemistry, Youngstown State University, Youngstown, Ohio 44555, United States;* orcid.org/0000-0002-2407-8262; Email: dtgenna@ysu.edu

Authors

Caleb J. Tatebe − *Department of Chemistry, Youngstown State University, Youngstown, Ohio 44555, United States;* orcid.org/0000-0002-7817-388X

Saidah Yusuf − *Department of Chemistry, Youngstown State University, Youngstown, Ohio 44555, United States*

Michael K. Bellas − *Department of Chemistry, Youngstown State University, Youngstown, Ohio 44555, United States*

Matthias Zeller − *Department of Chemistry, Purdue University, West Lafayette, Indiana 47907, United States;* orcid.org/0000-0002-3305-852X

Christopher Arntsen − *Department of Chemistry, Youngstown State University, Youngstown, Ohio 44555, United States*

Complete contact information is available at: https://pubs.acs.org/10.1021/acs.cgd.1c00766

Notes

The authors declare no competing financial interest.

■ ACKNOWLEDGMENTS

We thank Professors Jeremy Feldblyum and Alan Chen (SUNY Albany) for helpful discussions. This research was funded by NSF Grant DMRRUI: 1807462. The X-ray diffractometer was funded by NSF Grant DMR 1337296. This work was supported in part by an allocation of computing time from the Ohio Supercomputer Center.

■ REFERENCES

(1) Seth, S.; Matzger, A. J. Metal−Organic Frameworks: Examples, Counterexamples, and an Actionable Definition. *Cryst. Growth Des.* **2017**, *17*, 4043−4048.

(2) D'Alessandro, D. M. Exploiting redox activity in metal−organic frameworks: concepts, trends and perspectives. *Chem. Commun.* **2016**, *52*, 8957−8971.

(3) Goetjen, T. A.; Liu, J.; Wu, Y.; Sui, J.; Zhang, X.; Hupp, J. T.; Farha, O. K. Metal−organic framework (MOF) materials as polymerization catalysts: a review and recent advances. *Chem. Commun.* **2020**, *56*, 10409−10418.

(4) Thorarinsdottir, A. E.; Harris, T. D. Metal−Organic Framework Magnets. *Chem. Rev.* **2020**, *120*, 8716−8789.

(5) Islamoglu, T.; Chen, Z.; Wasson, M. C.; Buru, C. T.; Kirlikovali, K. O.; Afrin, U.; Mian, M. R.; Farha, O. K. Metal−Organic Frameworks against Toxic Chemicals. *Chem. Rev.* **2020**, *120*, 8130−8160.

(6) Rojas, S.; Horcajada, P. Metal−Organic Frameworks for the Removal of Emerging Organic Contaminants in Water. *Chem. Rev.* **2020**, *120*, 8378−8415.

(7) Wu, M.-X.; Yang, Y.-W. Metal−Organic Framework (MOF)-Based Drug/Cargo Delivery and Cancer Therapy. *Adv. Mater.* **2017**, *29*, 1606134.

(8) Bu, F.; Lin, Q.; Zhai, Q.-G.; Bu, X.; Feng, P. Charge-tunable indium−organic frameworks built from cationic, anionic, and neutral building blocks. *Dalton Trans* **2015**, *44*, 16671−16674.

(9) Zheng, S.-T.; Wu, T.; Chou, C.; Fuhr, A.; Feng, P.; Bu, X. Development of Composite Inorganic Building Blocks for MOFs. *J. Am. Chem. Soc.* **2012**, *134*, 4517−4520.

(10) Hosono, N.; Kitagawa, S. Modular Design of Porous Soft Materials via Self-Organization of Metal−Organic Cages. *Acc. Chem. Res.* **2018**, *51*, 2437−2446.

(11) Chen, J.; Shen, K.; Li, Y. Greening the Processes of Metal−Organic Framework Synthesis and their Use in Sustainable Catalysis. *ChemSusChem* **2017**, *10*, 3165−3187.

(12) Bosch, M.; Yuan, S.; Rutledge, W.; Zhou, H.-C. Stepwise Synthesis of Metal−Organic Frameworks. *Acc. Chem. Res.* **2017**, *50*, 857−865.

(13) Férey, G.; Haouas, M.; Loiseau, T.; Taulelle, F. Nanoporous Solids: How Do They Form? An In Situ Approach. *Chem. Mater.* **2014**, *26*, 299−309.

(14) Marshall, C. R.; Staudhammer, S. A.; Brozek, C. K. Size control over metal−organic framework porous nanocrystals. *Chem. Sci.* **2019**, *10*, 9396−9408.

(15) Armstrong, M. R.; Senthilnathan, S.; Balzer, C. J.; Shan, B.; Chen, L.; Mu, B. Particle size studies to reveal crystallization mechanisms of the metal organic framework HKUST-1 during sonochemical synthesis. *Ultrason. Sonochem.* **2017**, *34*, 365−370.

(16) Webber, T. E.; Desai, S. P.; Combs, R. L.; Bingham, S.; Lu, C. C.; Penn, R. L. Size Control of the MOF NU-1000 through Manipulation of the Modulator/Linker Competition. *Cryst. Growth Des.* **2020**, *20*, 2965−2972.

(17) Haouas, M.; Volkringer, C.; Loiseau, T.; Férey, G.; Taulelle, F. In Situ NMR, Ex Situ XRD and SEM Study of the Hydrothermal Crystallization of Nanoporous Aluminum Trimesates MIL-96, MIL-100, and MIL-110. *Chem. Mater.* **2012**, *24*, 2462−2471.

(18) Embrechts, H.; Kriesten, M.; Ermer, M.; Peukert, W.; Hartmann, M.; Distaso, M. Role of Prenucleation Building Units in Determining Metal−Organic Framework MIL-53(Al) Morphology. *Cryst. Growth Des.* **2020**, *20*, 3641−3649.

(19) Embrechts, H.; Kriesten, M.; Ermer, M.; Peukert, W.; Hartmann, M.; Distaso, M. In situ Raman and FTIR spectroscopic study on the formation of the isomers MIL-68(Al) and MIL-53(Al). *RSC Adv.* **2020**, *10*, 7336−7348.

(20) Embrechts, H.; Kriesten, M.; Hoffmann, K.; Peukert, W.; Hartmann, M.; Distaso, M. Elucidation of the Formation Mechanism of Metal−Organic Frameworks via in-Situ Raman and FTIR Spectroscopy under Solvothermal Conditions. *J. Phys. Chem. C* **2018**, *122*, 12267−12278.

(21) Ren, J.; Musyoka, N. M.; Langmi, H. W.; North, B. C.; Mathe, M.; Pang, W.; Wang, M.; Walker, J. In-situ IR monitoring of the formation of Zr-fumarate MOF. *Appl. Surf. Sci.* **2017**, *404*, 263−267.
(22) Ren, J.; Musyoka, N. M.; Langmi, H. W.; Walker, J.; Mathe, M.; Liao, S. In-situ IR monitoring to probe the formation of structural defects in Zr-fumarate metal−organic framework (MOF). *Polyhedron* **2018**, *153*, 205−212.
(23) Pichon, A.; Lazuen-Garay, A.; James, S. L. Solvent-free synthesis of a microporous metal−organic framework. *CrystEngComm* **2006**, *8*, 211−214.
(24) Friščić, T. Supramolecular concepts and new techniques in mechanochemistry: cocrystals, cages, rotaxanes, open metal−organic frameworks. *Chem. Soc. Rev.* **2012**, *41*, 3493−3510.
(25) Klimakow, M.; Klobes, P.; Thünemann, A. F.; Rademann, K.; Emmerling, F. Mechanochemical Synthesis of Metal−Organic Frameworks: A Fast and Facile Approach toward Quantitative Yields and High Specific Surface Areas. *Chem. Mater.* **2010**, *22*, 5216−5221.
(26) Yuan, W.; O'Connor, J.; James, S. L. Mechanochemical synthesis of homo- and hetero-rare-earth(iii) metal−organic frameworks by ball milling. *CrystEngComm* **2010**, *12*, 3515−3517.
(27) Forgan, R. S. Modulated self-assembly of metal−organic frameworks. *Chem. Sci.* **2020**, *11*, 4546−4562.
(28) Zhang, W.-Q.; Zhang, W.-Y.; Wang, R.-D.; Ren, C.-Y.; Li, Q.-Q.; Fan, Y.-P.; Liu, B.; Liu, P.; Wang, Y.-Y. Effect of Coordinated Solvent Molecules on Metal Coordination Sphere and Solvent-Induced Transformations. *Cryst. Growth Des.* **2017**, *17*, 517−526.
(29) Díaz-Torres, R.; Alvarez, S. Coordinating ability of anions and solvents towards transition metals and lanthanides. *Dalton Trans* **2011**, *40*, 10742−10750.
(30) Hausdorf, S.; Baitalow, F.; Seidel, J.; Mertens, F. O. R. L. Gaseous Species as Reaction Tracers in the Solvothermal Synthesis of the Zinc Oxide Terephthalate MOF-5. *J. Phys. Chem. A* **2007**, *111*, 4259−4266.
(31) Hausdorf, S.; Wagler, J.; Moβig, R.; Mertens, F. O. R. L. Proton and Water Activity-Controlled Structure Formation in Zinc Carboxylate-Based Metal Organic Frameworks. *J. Phys. Chem. A* **2008**, *112*, 7567−7576.
(32) Burrows, A. D.; Cassar, K.; Friend, R. M. W.; Mahon, M. F.; Rigby, S. P.; Warren, J. E. Solvent hydrolysis and templating effects in the synthesis of metal−organic frameworks. *CrystEngComm* **2005**, *7*, 548−550.
(33) Jin, S.; McKee, V.; Nieuwenhuyzen, M.; Robinson, W. T.; Wilkins, C. J. Evidence on ligand strengths from the crystal structures of $[InCl_3(dmf)_3]$, $[InCl_3(dma)_3]$, $[\{InCl_3(PhCHO)_3\}_2]\cdot PhCHO$ and $[InCl_3(PhCOMe)_2]$ from dimethylformamide (dmf), dimethylacetamide (dma), benzaldehyde and acetophenone. *J. Chem. Soc., Dalton Trans.* **1993**, 3111−3116.
(34) Brozek, C. K.; Michaelis, V. K.; Ong, T.-C.; Bellarosa, L.; López, N.; Griffin, R. G.; Dincă, M. Dynamic DMF Binding in MOF-5 Enables the Formation of Metastable Cobalt-Substituted MOF-5 Analogues. *ACS Cent. Sci.* **2015**, *1*, 252−260.
(35) Atzori, C.; Shearer, G. C.; Maschio, L.; Civalleri, B.; Bonino, F.; Lamberti, C.; Svelle, S.; Lillerud, K. P.; Bordiga, S. Effect of Benzoic Acid as a Modulator in the Structure of UiO-66: An Experimental and Computational Study. *J. Phys. Chem. C* **2017**, *121*, 9312−9324.
(36) Valenzano, L.; Civalleri, B.; Chavan, S.; Bordiga, S.; Nilsen, M. H.; Jakobsen, S.; Lillerud, K. P.; Lamberti, C. Disclosing the Complex Structure of UiO-66 Metal Organic Framework: A Synergic Combination of Experiment and Theory. *Chem. Mater.* **2011**, *23*, 1700−1718.
(37) Mihaly, J. J.; Tatebe, C. J.; Amirmokhtari, N.; DeSanto, M. J.; Zeller, M.; Genna, D. T. Halide Directed Synthesis of an In-Derived Metal−Organic Framework with Two Unique Metal Centers and Isolation of Its Potential Synthetic Precursor. *Cryst. Growth Des.* **2019**, *19*, 6053−6057.
(38) Mihaly, J. J.; Zeller, M.; Genna, D. T. Ion-Directed Synthesis of Indium-Derived 2,5-Thiophenedicarboxylate Metal−Organic Frameworks: Tuning Framework Dimensionality. *Cryst. Growth Des.* **2016**, *16*, 1550−1558.
(39) Springer, S. E.; Mihaly, J. J.; Amirmokhtari, N.; Crom, A. B.; Zeller, M.; Feldblyum, J. I.; Genna, D. T. Framework Isomerism in a Series of btb-Containing In-Derived Metal−Organic Frameworks. *Cryst. Growth Des.* **2019**, *19*, 3124−3129.
(40) Yu, J.; Cui, Y.; Wu, C.; Yang, Y.; Wang, Z.; O'Keeffe, M.; Chen, B.; Qian, G. Second-Order Nonlinear Optical Activity Induced by Ordered Dipolar Chromophores Confined in the Pores of an Anionic Metal−Organic Framework. *Angew. Chem., Int. Ed.* **2012**, *51*, 10542−10545.
(41) Cho, J.-S.; Cho, H.-G. $InCl_4^-$ Observed in the Raman Spectra of Deuterated Acetonitrile Containing $InCl_3$. *J. Korean Chem. Soc.* **2007**, *51*, 287−290.
(42) McGarvey, B. R.; Trudell, C. O.; Tuck, D. G.; Victoriano, L. Coordination compounds of indium. 37. Indium-115 NMR studies of anionic indium species in nonaqueous solution. *Inorg. Chem.* **1980**, *19*, 3432−3436.
(43) Cho, J.-S.; Cho, H.-G. Variation in IR and Raman Spectra of CD_3CN upon Solvation of $InCl_3$ in CD_3CN: Distinctive Blue Shifts, Coordination Number, Donor-Acceptor Interaction, and Solvated Species. *Bull. Korean Chem. Soc.* **2009**, *30*, 803−809.
(44) Chai, J.-D.; Head-Gordon, M. Long-range corrected hybrid density functionals with damped atom−atom dispersion corrections. *Phys. Chem. Chem. Phys.* **2008**, *10*, 6615−6620.
(45) Minenkov, Y.; Singstad, Å.; Occhipinti, G.; Jensen, V. R. The accuracy of DFT-optimized geometries of functional transition metal compounds: a validation study of catalysts for olefin metathesis and other reactions in the homogeneous phase. *Dalton Trans* **2012**, *41*, 5526−5541.
(46) Chiodo, S.; Russo, N.; Sicilia, E. LANL2DZ basis sets recontracted in the framework of density functional theory. *J. Chem. Phys.* **2006**, *125*, 104107.
(47) Woodward, L. A.; Taylor, M. J. 865. Raman effect and solvent extraction. Part II. Spectra of the tetrachloroindate and tetrachloroferrate ions. *J. Chem. Soc.* **1960**, 4473−4477.
(48) Mathur, M. S.; Ho, J. H. K.; Tabisz, G. C. Raman Study of $InCl_3$. *Spectrosc. Lett.* **1981**, *14*, 395−404.
(49) Details of which as it relates to the entire mechanism of formation of the MOF will be forthcoming in a separate manuscript.
(50) Maria, P. C.; Gal, J. F. A Lewis basicity scale for nonprotogenic solvents: enthalpies of complex formation with boron trifluoride in dichloromethane. *J. Phys. Chem.* **1985**, *89*, 1296−1304.
(51) Haynes, W. M.; Linde, D. R.; Bruno, T. J. *CRC Handbook of Chemistry and Physics: a ready-reference book of chemical and physical data.*, 97th ed.; CRC Press: 2016.

https://doi.org/10.1021/acs.cgd.1c00766
Cryst. Growth Des. 2021, 21, 6840−6846